ACT460 Final Project

Aparna Rai *, Zaid Tayeh†, Kabir Ben Nefla‡

December 1, 2025

Abstract

In this project, we study the pricing and risk sensitivities of several path-dependent options under the Black–Scholes model. We focus on arithmetic-average and geometric-average Asian call options as well as an up-and-out barrier call option. Monte Carlo simulation is used extensively to estimate option prices and Greeks, with both finite-difference and pathwise estimators. Analytic formulas for the geometric Asian call and the up-and-out call (from standard references) are compared against Monte Carlo estimates. We discuss parameter sensitivities, discretization effects, and the relative efficiency of different Greek estimation methods.

1 Introduction

1.1 Background and Motivation

Path-dependent options are derivatives whose payoffs depend on the entire path of the underlying asset price over time, rather than only on its terminal value. Common examples include Asian options (which depend on averages of prices) and barrier options (which depend on whether a barrier level is breached during the life of the option).

In actuarial and financial practice, such products arise in structured notes, risk management, and investment strategies. Their valuation typically requires numerical methods, especially when no closed-form solution is available.

1.2 Objectives

The main objectives of this project are:

1. To price an arithmetic-average Asian call option using Monte Carlo simulation and investigate the impact of model parameters (initial price, volatility, interest rate, maturity) on the option price.

2. To study discretization effects associated with monitoring frequency and time-stepping.

3. To estimate the Greeks (delta, vega, rho) of the arithmetic Asian call using both finite-difference and pathwise estimators and compare their performance.

4. To derive and implement a closed-form solution for the geometric-average Asian call and validate it against Monte Carlo estimates.

5. To describe, simulate, and analytically price an up-and-out call option (Option 3), comparing Monte Carlo estimates with a closed-form barrier option formula.

---

*(1006719204 a.rai@mail.utoronto.ca)
†(1008438585 zaid.tayeh@mail.utoronto.ca)
‡(1012873641 kabir.bennefla@mail.utoronto.ca)

1.3 Structure of the Report

The remainder of the report is organized as follows. Section 2 introduces the Black–Scholes model and our Monte Carlo simulation framework. Section 3 analyzes the arithmetic-average Asian call, including parameter sensitivity, discretization effects, and Greek estimation. Section 4 focuses on the geometric-average Asian call and its closed-form solution. Section 5 studies the up-and-out barrier call option. Section 6 concludes with a summary of findings and possible extensions. Technical derivations and additional tables/figures are provided in the appendices.

2 Model Setup and Simulation Framework

2.1 Black–Scholes Dynamics

For the purpose of pricing options We assume that the underlying asset price $(S_t)_{0 \leq t \leq T}$ follows the Black–Scholes model under the risk-neutral measure:

$$dS_t = rS_t \, dt + \sigma S_t \, dW_t, \tag{1}$$

where r is the continuously compounded risk-free interest rate, $\sigma > 0$ is the volatility, and $(W_t)_{t \geq 0}$ is a standard Brownian motion.

The exact solution of (1) is

$$S_t = S_0 \exp\left(\left(r - \frac{1}{2}\sigma^2\right)t + \sigma W_t\right), \tag{2}$$

where S_0 is the initial asset price.

Throughout the project, we use the following baseline parameters:

$$S_0 = 100, \quad K = 100, \quad r = 0.05, \quad \sigma = 0.4, \quad T = 1. \tag{3}$$

2.2 Discrete Time Grid and Monte Carlo Simulation

We discretize the interval $[0, T]$ into m steps with

$$0 = t_0 < t_1 < \cdots < t_m = T, \qquad \Delta t = \frac{T}{m}.$$

Using the exact solution (2), the asset price at step $k + 1$ can be simulated as

$$S_{t_{k+1}} = S_{t_k} \exp\left(\left(r - \frac{1}{2}\sigma^2\right)\Delta t + \sigma\sqrt{\Delta t}Z_{k+1}\right), \tag{4}$$

where $Z_{k+1} \sim N(0, 1)$ are i.i.d.

For each experiment, we simulate N independent sample paths of the process $(S_{t_k})_{k=0,\ldots,m}$. The discounted payoff of interest is computed for each path, and the Monte Carlo estimator of the option price is given by

$$\hat{V}_N = \frac{1}{N}\sum_{j=1}^{N}\Pi^{(j)}, \tag{5}$$

where $\Pi^{(j)}$ is the discounted payoff for path j.

The corresponding Monte Carlo standard error is

$$\widehat{\mathrm{SE}}(\hat{V}_N) = \sqrt{\frac{1}{N(N-1)}\sum_{j=1}^{N}\left(\Pi^{(j)} - \hat{V}_N\right)^2}, \tag{6}$$

and an approximate 95% confidence interval is

$$\hat{V}_N \pm 1.96\,\widehat{\mathrm{SE}}(\hat{V}_N).$$

2.3 Implementation Overview

All computations are carried out in Python using Jupyter notebooks. A reusable function simulates GBM paths via (4). Separate functions implement the payoffs of the arithmetic Asian call, geometric Asian call, and up-and-out Call options. Additional helper functions perform parameter sweeps and Greek estimation.

3 Arithmetic-Average Asian Call

3.1 Definition and Payoff (Q1)

Let $0 < t_1 < \cdots < t_m = T$ be monitoring times. The arithmetic average of the underlying prices is

$$\bar{S}_A = \frac{1}{m} \sum_{i=1}^{m} S_{t_i}. \tag{7}$$

The payoff of an arithmetic-average Asian call with strike K and maturity T is

$$\Pi_A = e^{-rT} \max(\bar{S}_A - K, 0). \tag{8}$$

No simple closed-form expression for the price is available under the standard Black–Scholes model, so we rely on Monte Carlo methods.

3.2 Monte Carlo Pricing Method (Q1)

We simulate N paths of the GBM process using (4), compute the arithmetic average (7) for each path, and evaluate the discounted payoff (8). The Monte Carlo price estimator is given by (5).
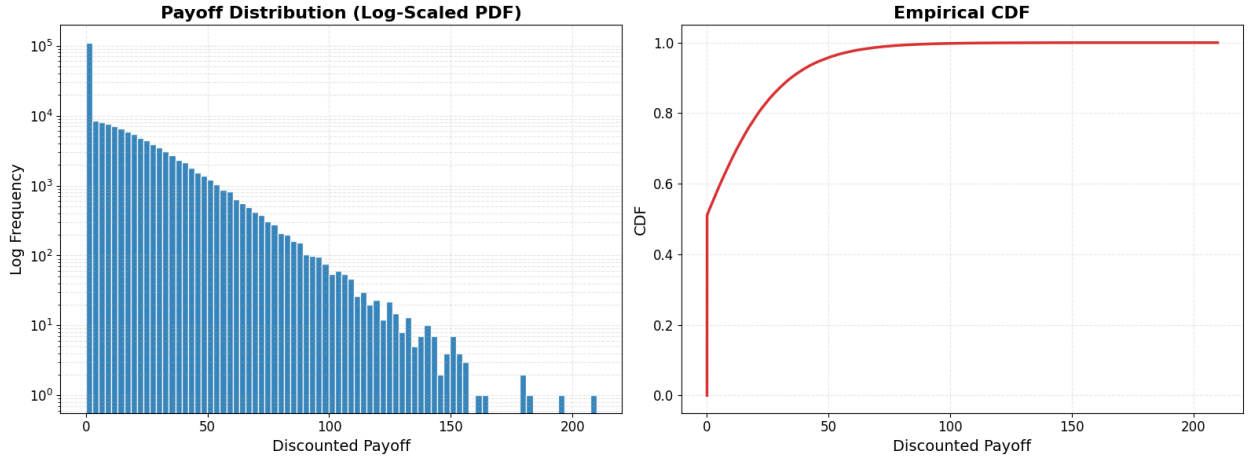

Figure 1: **Left:** Log-scaled histogram of discounted payoffs for the arithmetic-average Asian call. **Right:** Empirical cumulative distribution function (CDF) of the same payoffs. The log scale reveals the long right tail and the heavy mass at zero that is not visible under a linear scale.

Table 1: Placeholder: Monte Carlo estimate of arithmetic Asian call price at baseline parameters.

	Estimate	Std. Error	95% CI
Monte Carlo	10.176	0.0367	[10.104,10.248]

We notice that the payoff distribution is highly skewed, with a large mass at zero and a long right tail, as shown in Figure 1. Despite this skewness, the Monte Carlo estimator is stable: the price estimate of 10.18

3

has a small standard error (0.0367) and a tight 95% confidence interval. This indicates that the simulation with $N = 200{,}000$ paths provides a reliable estimate of the arithmetic Asian call value under the baseline parameters.

3.3 Parameter Sensitivity Analysis (Q2)

We now study the effect of model parameters on the Asian arithmetic call price by varying one parameter at a time while holding others fixed at their baseline values (3).

Parameter	Value
S_0	100.0
K	100.0
r	0.05
σ	0.4
T	1.0
m	252
Arithmetic Asian (CV)	10.1589 ± 0.0088 (VR $\approx 211.5\times$)
European Call (BS)	18.0230
Geometric Asian (disc.)	9.3965

Table 2: Baseline parameter values and option prices.

3.3.1 Sensitivity to Initial Price S_0

We consider a grid $S_0 \in \{60, 80, 90, 100, 110, 120, 140\}$ and estimate the option price for each value.

S_0	Price	95% CI
60	0.1541	[0.1505, 0.1576]
80	2.2949	[2.2888, 2.3011]
90	5.3588	[5.3514, 5.3661]
100	10.1589	[10.1502, 10.1677]
110	16.5796	[16.5686, 16.5905]
120	24.2837	[24.2710, 24.2964]
140	42.0043	[41.9880, 42.0206]

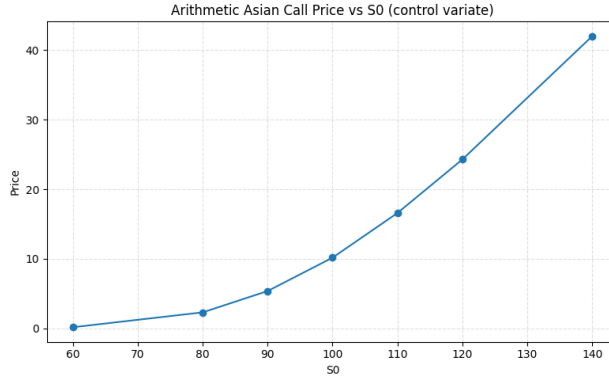Table 3: S_0 sweep for Asian option price.

Figure 2: Arithmetic Asian call price as a function of S_0.

We observe that the arithmetic Asian call price increases monotonically in S_0, as expected for a call option. For very low initial prices (e.g., $S_0 = 60$) the option is deeply out-of-the-money for most paths, so the average rarely exceeds the strike and the price is close to zero. As S_0 moves through and above the at-the-money region ($S_0 \approx 100$), the option quickly becomes more likely to finish in-the-money and the price grows sharply. Over the range considered, the price–S_0 relationship is smooth and close to linear, reflecting a relatively stable delta, but with some curvature due to the convexity of the payoff. Compared with a European call, the averaging in the payoff dampens short-term path fluctuations, leading to a slightly smoother dependence on S_0.

3.3.2 Sensitivity to Strike Price K

We next consider varied values of $K \in \{60, 80, 90, 100, 110, 120, 140\}$ and estimate the option price for each value.

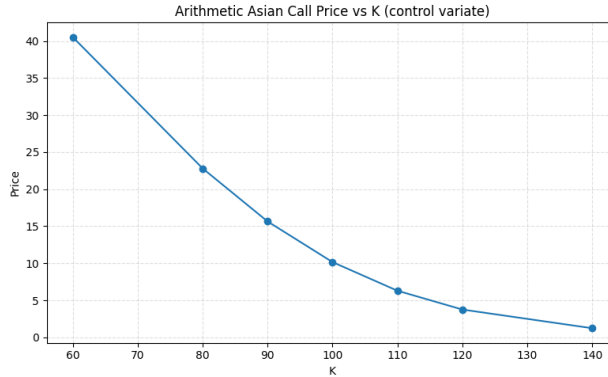| K	Price	95% CI
60	40.5033	[40.4908, 40.5158]
80	22.7930	[22.7821, 22.8038]
90	15.6423	[15.6323, 15.6524]
100	10.1589	[10.1502, 10.1677]
110	6.2949	[6.2867, 6.3031]
120	3.7565	[3.7487, 3.7643]
140	1.2362	[1.2290, 1.2433]

Table 4: K sweep for Asian option price.

Figure 3: Arithmetic Asian call price as a function of K.

The option value decreases monotonically as the strike K increases, which is consistent with basic no-arbitrage intuition: a higher strike makes it harder for the averaged price to exceed K, reducing both the probability and magnitude of positive payoffs. The steepest decline occurs around the at-the-money region (K near 100), where small changes in K significantly alter the proportion of paths that end in-the-money. For very high strikes (e.g., $K = 140$), the price approaches zero, reflecting a deeply out-of-the-money contract whose payoff is rarely triggered. Again, the use of the arithmetic average smooths the dependence on K relative to a European call, since extreme spikes in the underlying contribute less to the payoff.

3.3.3 Sensitivity to Volatility σ

Similarly, we vary volatility $\sigma \in \{0.10, 0.20, 0.30, 0.40, 0.60\}$ and estimate the price.

The Asian call price increases with volatility σ, mirroring the standard behaviour of call options: greater volatility increases the dispersion of the underlying paths and, by convexity of the payoff, raises the expected

σ	Price	95% CI
0.1	3.6531	[3.6525, 3.6537]
0.2	5.7791	[5.7768, 5.7813]
0.3	7.9649	[7.9600, 7.9697]
0.4	10.1589	[10.1502, 10.1677]
0.6	14.5199	[14.4983, 14.5416]

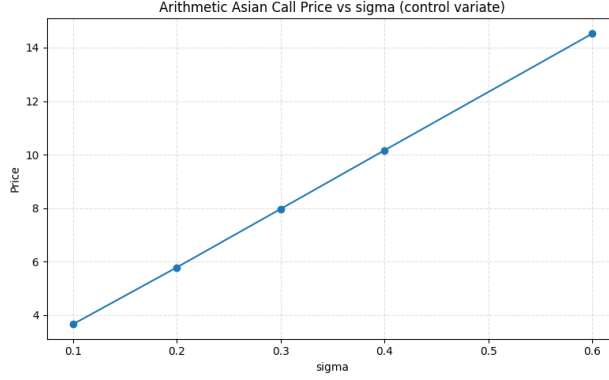Table 5: σ sweep for Asian option price.

Figure 4: Arithmetic Asian call price as a function of volatility σ.

payoff. For low volatility ($\sigma = 0.1$), the underlying stays close to its drift path and the average is relatively predictable, leading to a modest option value. As σ grows, there is a higher chance that at least part of the path takes large upward excursions, lifting the arithmetic average well above the strike even though some paths also fall far below it. This convexity effect dominates the discounting and the averaging, so the price rises markedly from about 3.65 to 14.52 over the range considered.

3.3.4 Sensitivity to Interest Rate r

We vary r over a suitable range, $r \in \{0.00, 0.02, 0.05, 0.10\}$.

r	Price	95% CI
0	9.1982	[9.1900, 9.2064]
0.02	9.5789	[9.5705, 9.5873]
0.05	10.1589	[10.1502, 10.1677]
0.1	11.1484	[11.1388, 11.1579]

Table 6: r sweep for Asian option price.

The Asian call price is increasing in the risk-free rate r, which is consistent with risk-neutral pricing: under the risk-neutral measure, the drift of S_t is r, so a higher r pushes the expected level of the underlying (and hence its average) upward over time. At the same time, the discount factor e^{-rT} becomes smaller as r increases, but for a call option on a non-dividend-paying asset the positive effect on the expected average typically outweighs the stronger discounting. This net effect is clearly seen in the results: moving from $r = 0$ to $r = 0.10$ increases the price from approximately 9.20 to 11.15. Thus, the qualitative dependence on r is similar to that of a European call, although the averaging again moderates the magnitude of the response.
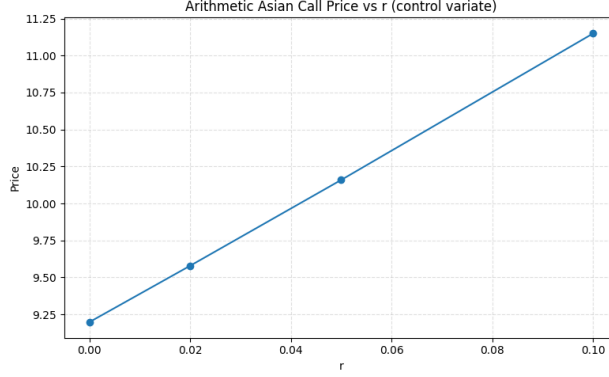
6

Figure 5: Arithmetic Asian call price as a function of interest rate r.

3.3.5 Sensitivity to Maturity T

We vary the time to maturity T, $T \in \{0.25, 0.50, 1.00, 2.00\}$ and note how different maturities influence the average and payoff.

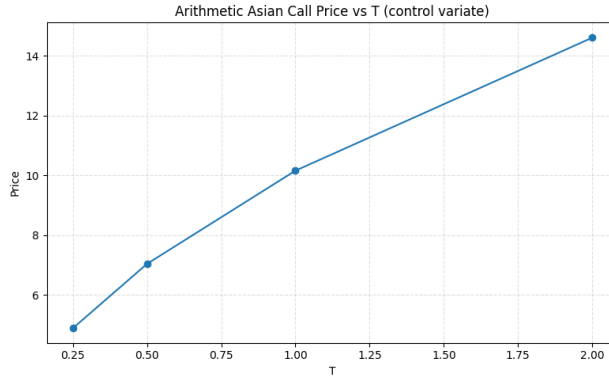| T	Price	95% CI
0.25	4.8930	$[4.8911,\ 4.8950]$
0.5	7.0447	$[7.0406,\ 7.0487]$
1	10.1589	$[10.1502,\ 10.1677]$
2	14.6022	$[14.5826,\ 14.6219]$

Table 7: T sweep for Asian option price.

Figure 6: Arithmetic Asian call price as a function of maturity T.

The option value increases with the time to maturity T. A longer horizon allows more time for the underlying to experience favourable upward movements, which can lift the arithmetic average above the strike, even if some parts of the path are below K. For very short maturities (e.g., $T = 0.25$), there is limited opportunity for the average to differ much from the initial level, so the option value is relatively low. As T grows from 0.25 to 2, the price rises steadily from about 4.89 to 14.60, despite the stronger discounting e^{-rT}, indicating that the extra time value dominates. The incremental gain in price appears to taper off somewhat, reflecting diminishing marginal benefit from very long maturities.

7

3.3.6 Sensitivity to Trading Periods m

We vary the number of trading days in a period m, $m \in \{12, 52, 126, 252, 504\}$ and analyze the effect on the average and payoff.

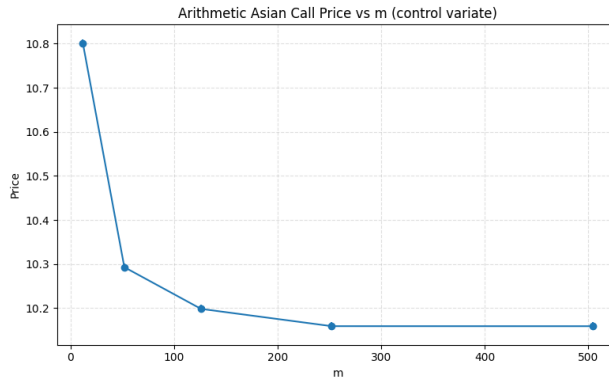| m	Price	95% CI
12	10.8008	[10.7913, 10.8103]
52	10.2928	[10.2838, 10.3018]
126	10.1982	[10.1892, 10.2071]
252	10.1589	[10.1502, 10.1677]
504	10.1589	[10.1496, 10.1681]

Table 8: m sweep for Asian option price.

Figure 7: Arithmetic Asian call price as a function of trading periods m.

Varying the number of monitoring dates m reveals a clear discretization effect. For coarse monitoring (e.g., $m = 12$), the arithmetic average places relatively more weight on later times, where the expected level of S_t is higher due to positive drift, leading to a slightly larger average and thus a higher option value. As m increases, additional intermediate points are included in the average, giving more weight to earlier times when the expected price is lower; this pulls the average down and reduces the option price. The results show the price decreasing from about 10.80 at $m = 12$ to 10.16 around $m = 252$, after which it essentially stabilizes, indicating convergence to the continuous-monitoring limit. This behaviour highlights that the choice of monitoring frequency can introduce a small but systematic bias if one approximates a continuously averaged contract with a coarse discrete grid.

3.4 Discretization Error Study (Q3)

In this section we investigate the effect of time discretization on the estimated price of the arithmetic-average Asian call. Following project requirements, we compare **three** time-discretization schemes introduced in the course:

1. Euler–Maruyama scheme (order 1/2 strong).

2. Milstein scheme (order 1 strong).

3. Second-order weak Taylor scheme (order 2 weak).

Each scheme produces a different approximation to the SDE dynamics, and therefore a different approximation of the average price and payoff.

3.4.1 Discretization Schemes

Let $\Delta t = T/N$ and $Z_k \sim N(0,1)$. When pricing the Asian call option, we have to consider that the underlying asset follows a continuous time SDE given by $dS_t = \mu(S_t, t)dt + \sigma(S_t, t)dW_t$. When running a simulation for this, we can only run it using a discrete time approximation. This is the general idea behind Monte-Carlo pricing simulations. Fundamentally, all the discretization schemes are:

1. Breaking the interval $[0, T]$ into N time steps.

2. Approximating the random evolution of S_t.

3. Accumulates the approximations from (2) which creates a discrete time approximation of the whole sample path.

4. Using the simulated paths to compute the payoff of the Asian call.

Let us explore the details of all three discretization methods below.

1. Euler–Maruyama Scheme.
A general ito SDE has the form: $dX_t = a(t, X_t)dt + b(t, X_t)dW_t$, where a, b, and W_t are the drift, diffusion, and Brownian motion components, respectively. We can assume that a and b are constants under EM and that the Brownian increments are normally distributed with mean 0 and variance Δt. Thus, after integrating the SDE on both sides from t_k to t_{k+1} we arrive at: $X_{t_{k+1}} = X_{t_k} + a(t_k, X_{t_k})\Delta t + b(t_k, X_{t_k})\sqrt{\Delta t}Z_k$. EM has a weak convergence order 1 and a strong convergence order 0.5. For the Monte Carlo pricing, we only care about the weak order; this is fine when N is moderately large. For the arithmetic average Asian call, the payoff depends on all intermediate values. This makes EM sensitive to discretization bias, which tends to underestimate the average. Milstein and Second Order tend to reduce this bias.

2. Milstein Scheme.
The Milstein Scheme is the next level (in terms of numerical accuracy) on Euler Mauryama. EM approximates $X_{t_{k+1}}$ but ignores all higher order stochastic terms that arise from Ito's formula. Milstein's discretization is given by $X_{t_{k+1}} = X_{t_k} + a(t_k, X_{t_k})\Delta t + b(t_k, X_{t_k})\sqrt{\Delta t}Z_k + \frac{1}{2}b(t_k, X_{t_k})b'(t_k, X_{t_k})[(\Delta W_k)^2 - \Delta t]$. Milstein has strong convergence with order 1, which means the simulated paths are closer to the true paths. The added term (relative to EM) comes from the fact that BMs have quadratic variation $(dW_t)^2 = dt$. Ito's lemma expands the SDE to include terms with second-derivatives. Euler Maruyama drops these terms and Milstein restores the largest missing terms; this greatly improves path wise accuracy.
3. Second-Order Weak Taylor Scheme.
Instead of improving pathwise accuracy like Milstein, the Weak 2nd order Taylor Scheme improves expected values (better for option pricing). The Taylor scheme does this by adding extra drift and moment-catching terms, which is derived from the Taylor expansion of expectations. EM gives only weak order accuracy, meaning: $E[f(X_t)] = E[f(\hat{X}_t)] + O(\Delta t)$. This is not accurate unless Δt is small. Milstein improves path wise accuracy but does not improve weak accuracy beyond first order. To get a weak order 2, you need to reproduce the values of the first four moments of ΔW. The Taylor scheme adds terms that represent these moments.

3.4.2 Numerical Results

Table 9: Monte Carlo Prices using the discretization schemes.

Scheme	Price	Std. Error	Bias
Euler Maruyama	10.283273	0.052347	0.003237
Milstein	10.270711	0.052649	-0.009325
Second Order Weak Taylor	10.280333	0.052709	0.000296
Exact	10.280037	0.052710	0.000000

3.5 Greeks for the Arithmetic Asian Call (Q4)

3.5.1 Definitions and Greeks of Interest

Recall the arithmetic average $\bar{S}_A$ in (7) and the discounted payoff Π_A in (8). Denote the option price by $V(S_0, \sigma, r)$; the Greeks of interest are

$$\Delta = \frac{\partial V}{\partial S_0}, \tag{9}$$

$$\nu = \frac{\partial V}{\partial \sigma} \quad \text{(vega)}, \tag{10}$$

$$\rho = \frac{\partial V}{\partial r}. \tag{11}$$

We estimate these using both pathwise (PW) estimators and finite-difference (FD) estimators with common random numbers (CRN), and compare their variance, bias, and stability.

For Q4 we use the baseline parameters (3) with $m = 252$ monitoring dates. All prices and Greeks are computed by Monte Carlo simulation of the exact GBM step (4), with a fixed time grid, $N = 200{,}000$ base paths, and antithetic variates (effective 400,000 payoff samples). A fixed random seed is used for reproducibility. Here we work with the raw Monte Carlo estimator (no control variate), so the Q4 price estimate differs slightly from the variance-reduced estimate reported in the parameter sensitivity section.

Unless stated otherwise, 95% confidence intervals (CIs) are reported as

$$\text{estimate} \pm \text{half-width}, \qquad \text{half-width} = 1.96 \times \text{s.e.},$$

where the standard error is estimated from the Bessel-corrected sample variance and divided by $\sqrt{N_{\text{eff}}}$, with N_{eff} the effective number of paths (after antithetics).

3.5.2 Baseline Pathwise Estimates

Quantity	Estimate	95% CI (half-width)
Asian (arith) price	10.2274	0.0725
Δ (PW)	0.5665	0.0026
ν (PW)	22.1320	0.2072
ρ (PW)	19.5449	0.0902

Table 10: Baseline pathwise estimates for the arithmetic-average Asian call.

In our implementation we also check basic sign constraints on the Greeks (printed by the code): $\Delta \in (0, 1)$, $\nu > 0$, and $\rho > 0$. All three constraints are satisfied, which is consistent with the usual monotonicity properties of call option prices.

3.5.3 Bounds and Comparator Prices

Under GBM and the risk–neutral measure we can compute $\mathbb{E}[\bar{S}_A]$, and then construct simple bounds and comparators for the Asian price.

Quantity	Value
$\mathbb{E}[\bar{S}_A]$	102.5524
Jensen lower bound $e^{-rT}(\mathbb{E}[\bar{S}_A] - K)^+$	2.4279
Trivial upper bound $e^{-rT}\mathbb{E}[\bar{S}_A]$	97.5508
Geometric–Asian (closed form)	9.3965
European call (Black–Scholes)	18.0230

Table 11: Comparator values and bounds; satisfies Geometric $\leq$ Arithmetic $\leq$ European ($9.3965 \leq 10.2274 \leq 18.0230$).

The lower bound uses Jensen's inequality applied to the convex function $x \mapsto (x - K)^+$:

$$e^{-rT}\mathbb{E}[(\bar{S}_A - K)^+] \ \geq \ e^{-rT}(\mathbb{E}[\bar{S}_A] - K)^+.$$

The trivial upper bound follows from

$$(\bar{S}_A - K)^+ \leq \bar{S}_A \quad \Rightarrow \quad e^{-rT}\mathbb{E}[(\bar{S}_A - K)^+] \leq e^{-rT}\mathbb{E}[\bar{S}_A].$$

The simulated arithmetic price 10.2274 lies strictly between the geometric Asian price and the European call price, as expected.

3.5.4 Pathwise vs Finite Differences (CRN)

We next compare pathwise and FD estimators for Δ, ν, ρ. For each Greek, FD uses a central-difference approximation with bump sizes h_S, h_σ, h_r and common random numbers across all bumped runs.

Bumps (Δ, ν, ρ)	Greek	FD estimate	PW estimate	Within ~1–2 s.e.?
$(\,0.0005, 0.0005, 0.0005)$	Δ	0.5665	0.5665	Yes
	ν	22.1318	22.1320	Yes
	ρ	19.5455	19.5449	Yes
$(\,0.001, 0.001, 0.001)$	Δ	0.5665	0.5665	Yes
	ν	22.1318	22.1320	Yes
	ρ	19.5462	19.5449	Yes
$(\,0.005, 0.005, 0.005)$	Δ	0.5665	0.5665	Yes
	ν	22.1316	22.1320	Yes
	ρ	19.5439	19.5449	Yes

Table 12: FD vs pathwise across bump sizes, using common random numbers (CRN).

For all three bump sizes, the FD estimates agree with the pathwise estimates well within 1–2 standard errors. The corresponding FD–PW z-scores (not shown) are close to zero and comfortably inside the 95% acceptance band $|z| \leq 1.96$.

3.5.5 Convergence with the Number of Paths N

To check Monte Carlo convergence, we run the simulation at N and $2N$ base paths and compare the standard errors. For an i.i.d. estimator we expect the standard error to scale like $N^{-1/2}$, so the ratio of standard errors between N and $2N$ should be close to $\sqrt{2} \approx 1.414$.

s.e. ratio (N vs $2N$)	Price	Δ	ν	ρ
Observed	1.42	1.42	1.42	1.41
Reference value		$\sqrt{2} \approx 1.414$		

Table 13: Standard-error scaling check (should be close to $\sqrt{2}$).

The observed ratios (≈ 1.42) are numerically very close to $\sqrt{2} \approx 1.414$, which confirms that the estimators behave as expected under the usual Monte Carlo scaling s.e. $\propto N^{-1/2}$.

3.5.6 Model Checks: GBM Marginals

As a sanity check on the GBM simulation, we compare empirical and theoretical moments at a few times t.

t	$\mathbb{E}[S_t]$ (MC)	Theory	$\mathrm{Var}(\ln S_t/S_0)$ (MC)	Theory
0.25	101.277	101.258	0.0404	0.0400
0.50	102.561	102.532	0.0806	0.0800
1.00	105.153	105.127	0.1605	0.1600

Table 14: GBM moment checks at a few monitoring times.

The empirical means and log-variance estimates are very close to their theoretical values $S_0 e^{rt}$ and $\sigma^2 t$, indicating that the GBM simulation is correctly implemented.

3.5.7 Monitoring-Frequency Effect

We also study how the arithmetic Asian price varies with the monitoring frequency m, keeping T fixed. Intuitively, as m increases the average tracks the path more closely and the payoff becomes less like a European call.

m	Price	95% CI (half-width)
10	10.9360	0.1101
50	10.3509	0.1044
150	10.2131	0.1024
250	10.1620	0.1023
500	10.1559	0.1021

Table 15: Effect of monitoring frequency m on the arithmetic Asian price.

The price decreases as m increases, in line with the intuition that more frequent averaging reduces the effective upside relative to a European call, since occasional large spikes in S_t are averaged out more heavily.

3.5.8 Summary Diagnostics and Discussion

(a) Greeks (PW vs FD) with 95% CIs.

(b) FD vs PW z-scores across bump sizes.

(c) s.e. vs N (reference line $N^{-1/2}$).

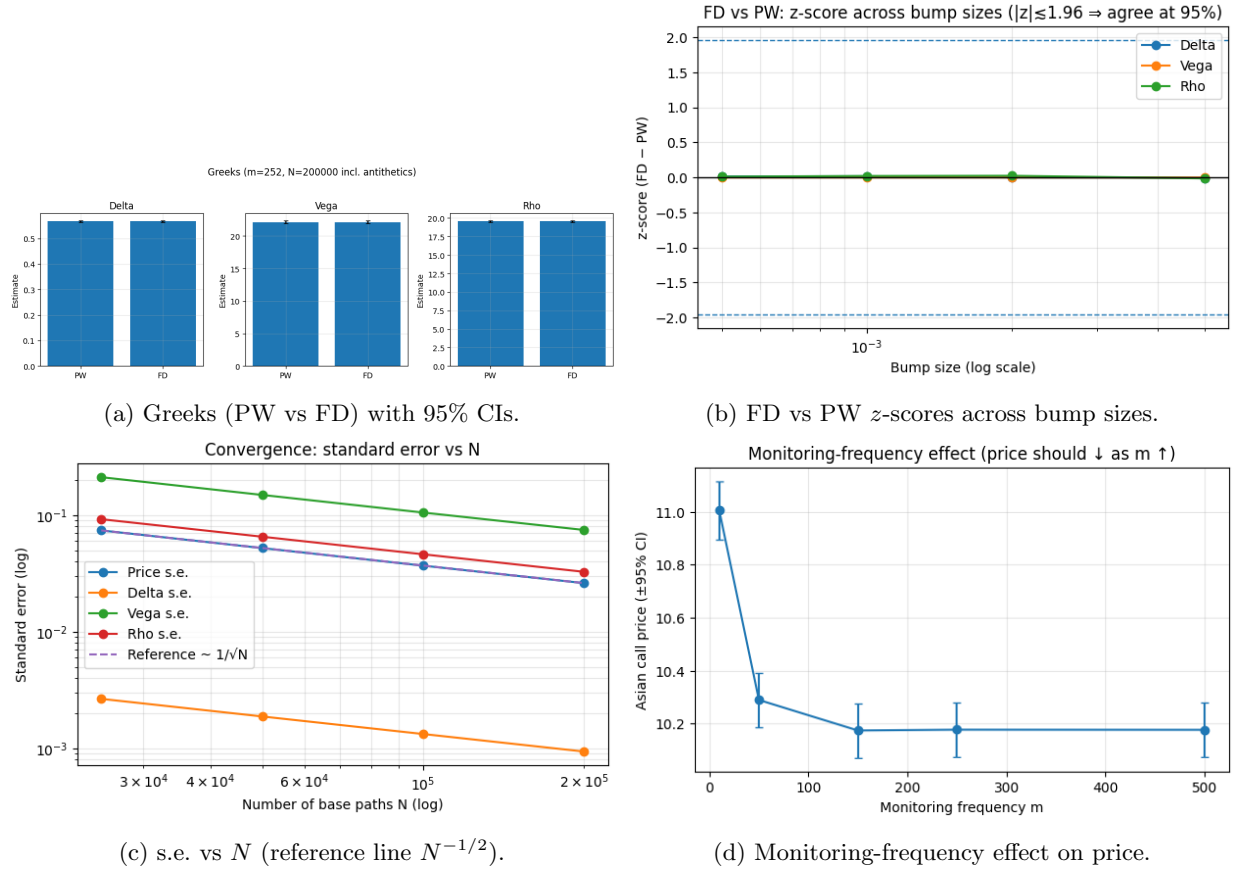

(d) Monitoring-frequency effect on price.

Figure 8: Overview of Q4 diagnostics. Panels are referenced in the text.

- **Variance.** Pathwise and FD estimators have statistically indistinguishable means. At $N = 200{,}000$ (antithetics), the tightest CI is for Δ (± 0.0026). The CIs for ν (± 0.2072) and ρ (± 0.0902) are wider but still reasonably tight.

- **Bias and stability.** Finite differences are stable for bumps 5×10^{-4}, 10^{-3}, and 5×10^{-3}: FD–PW z-scores (Figure 8b) are near zero and well within $|z| \leq 1.96$, so both approaches agree at the 95% level.

- **Efficiency.** Standard errors decay close to $1/\sqrt{N}$ (observed $N:2N$ ratios ≈ 1.42 vs. $\sqrt{2}$), as shown in Figure 8c. Antithetics improve precision; CRN removes most FD noise relative to PW, making FD nearly as efficient as the pathwise method at these settings.

Takeaway. Either estimator is acceptable here; the pathwise method is convenient for Δ, while CRN makes finite differences competitive across all Greeks.

4 Geometric-Average Asian Call (Q5)

4.1 Problem Setup

We now consider the geometric-average Asian call built on the same GBM

$$dS_t = rS_t\,dt + \sigma S_t\,dW_t,$$

with monitoring dates $0 < t_1 < \cdots < t_m = T$ and baseline parameters (3). The geometric average over the monitoring dates is

$$\tilde{S} = \left(\prod_{i=1}^{m} S_{t_i}\right)^{1/m}, \tag{12}$$

and the discounted payoff is

$$\Pi_G = e^{-rT}(\tilde{S} - K)^+. \tag{13}$$

Goal. Show that $\ln \tilde{S}$ is Gaussian under GBM and derive a closed-form (Black–Scholes–style) expression for

$$Y = e^{-rT}\,\mathbb{E}[(\tilde{S} - K)^+],$$

then verify the formula numerically using Monte Carlo simulation.

We emphasise that this is a *discrete* geometric average at the dates $\{t_i\}$; a continuous-time geometric average over $[0, T]$ leads to slightly different parameters.

4.2 Distribution of the Log-Geometric Average

The explicit GBM solution at monitoring time t_i is

$$S_{t_i} = S_0 \exp\!\big((r - \tfrac{1}{2}\sigma^2)t_i + \sigma W_{t_i}\big), \tag{14}$$

so

$$\ln \tilde{S} = \frac{1}{m}\sum_{i=1}^{m} \ln S_{t_i}$$

$$= \ln S_0 + \frac{1}{m}\sum_{i=1}^{m}\big((r - \tfrac{1}{2}\sigma^2)t_i + \sigma W_{t_i}\big). \tag{15}$$

Mean. Using $\mathbb{E}[W_{t_i}] = 0$, we obtain

$$\mu_G := \mathbb{E}[\ln \tilde{S}] = \ln S_0 + \frac{r - \frac{1}{2}\sigma^2}{m} \sum_{i=1}^{m} t_i. \tag{16}$$

For equally spaced monitoring $t_i = iT/m$,

$$\sum_{i=1}^{m} t_i = \frac{T(m+1)}{2} \quad \Rightarrow \quad \mu_G = \ln S_0 + \left(r - \tfrac{1}{2}\sigma^2\right) T \frac{m+1}{2m}. \tag{17}$$

Variance. Using $\mathrm{Cov}(W_{t_i}, W_{t_j}) = \min(t_i, t_j)$ we get

$$\sigma_G^2 := \mathrm{Var}(\ln \tilde{S}) = \frac{\sigma^2}{m^2} \sum_{i=1}^{m} \sum_{j=1}^{m} \min(t_i, t_j). \tag{18}$$

For $t_i = iT/m$,

$$\sum_{i=1}^{m} \sum_{j=1}^{m} \min(t_i, t_j) = \frac{T}{m} \sum_{i=1}^{m} \sum_{j=1}^{m} \min(i, j) = T \frac{(m+1)(2m+1)}{6}, \tag{19}$$

so

$$\sigma_G^2 = \sigma^2 T \frac{(m+1)(2m+1)}{6m^2}. \tag{20}$$

Therefore

$$\ln \tilde{S} \sim \mathcal{N}(\mu_G, \sigma_G^2) \quad \Longrightarrow \quad \tilde{S} \text{ is lognormal.} \tag{21}$$

4.3 Black–Scholes–Style Pricing Form

Define

$$\tilde{S}_0^{\mathrm{eff}} = e^{\mu_G}, \qquad \sigma_{\mathrm{eff}} = \sigma_G. \tag{22}$$

Then $\ln \tilde{S}$ is normal with mean μ_G and variance σ_{eff}^2, so a standard lognormal pricing argument yields

$$d_1 = \frac{\ln(\tilde{S}_0^{\mathrm{eff}}/K) + \frac{1}{2}\sigma_{\mathrm{eff}}^2}{\sigma_{\mathrm{eff}}}, \qquad d_2 = d_1 - \sigma_{\mathrm{eff}}. \tag{23}$$

The geometric-Asian call price is

$$Y = e^{-rT} \mathbb{E}[(\tilde{S} - K)^+] = e^{-rT} \left(\tilde{S}_0^{\mathrm{eff}} e^{\frac{1}{2}\sigma_{\mathrm{eff}}^2} \Phi(d_1) - K \Phi(d_2) \right), \tag{24}$$

where Φ is the standard normal CDF.

Equivalently, we can rewrite this as a Black–Scholes call with an effective "dividend yield" q_G:

$$C = S_0 e^{-q_G T} \Phi(d_1) - K e^{-rT} \Phi(d_2), \tag{25}$$

with

$$q_G = \frac{r(m-1)}{2m} + \frac{\sigma^2(m^2-1)}{12m^2}, \tag{26}$$

and the same d_1, d_2 as above. The parameter q_G is chosen so that

$$S_0 e^{(r-q_G)T} = \mathbb{E}[\tilde{S}] = e^{\mu_G + \frac{1}{2}\sigma_G^2}, \tag{27}$$

i.e. the effective forward on $\tilde{S}$ under this dividend yield matches its true expectation.

Remarks.

- The product of lognormal variables is lognormal because the logarithm of the product is a sum of normal variables.

- Monitoring is *discrete* at $\{t_i\}$; the parameters μ_G and σ_G^2 are computed from these specific dates.

4.4 Monte Carlo Verification

We now verify the analytic formula (24) by Monte Carlo simulation using the same GBM grid and baseline parameters as in the previous section, with $m = 252$ and $N = 200{,}000$ base paths with antithetics (effective 400,000 payoff samples). For each path we compute the geometric average $\tilde{S}$ and the discounted payoff $e^{-rT}(\tilde{S} - K)^+$, then estimate the price and its standard error.

Quantity	Analytic	MC (mean $\pm$ 95% half-width)	Abs. err.	% err
Price	9.3965	9.4541 $\pm$ 0.0674	0.0576	0.613

Table 16: Geometric-average Asian call ($m = 252$, $N = 200{,}000$ base paths with antithetics; effective 400,000 payoff samples).

The analytic value lies well within the 95% Monte Carlo confidence interval. The absolute error (≈ 0.058) is small relative to the CI half-width (≈ 0.067), and the percentage error is about 0.6%; the difference is not statistically significant at the 5% level.

Figure 9 illustrates the convergence of the Monte Carlo estimate to the analytic value as the number of paths increases. The mean estimate remains close to the analytic price, while the CI width decreases approximately at the $N^{-1/2}$ rate.
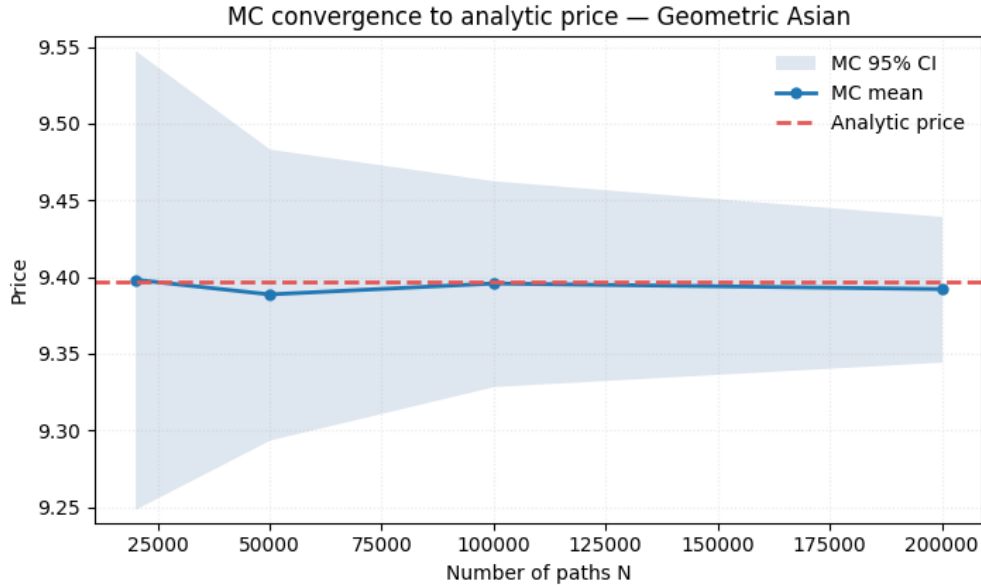

Figure 9: Monte Carlo convergence to the analytic price for the geometric-average Asian call.

Overall, the Monte Carlo results are fully consistent with the closed form, which validates both our derivation and our simulation code for the geometric-average Asian call.

5 Up-and-Out Call Option (Q6 – Option 3)

5.1 Contract Definition and Uses

An up-and-out call option is a European call option that immediately becomes worthless if the price of the underlying asset exceeds (or touches) a determined upper barrier level (B) at anytime before (or at) maturity. If the asset price reaches this barrier, then the payoff automatically becomes 0. If the barrier never hits, it behaves like a normal European call option.

$$
\text{Payoff} = \begin{cases} 0, & \text{if } \max_{0 \leq t \leq T} S_t \geq B, \\ (S_T - K)^+, & \text{otherwise.} \end{cases}
$$

Intuitively, an up-and-out call option must be cheaper than a vanilla European call option because there is now an upper bound for the price of the underlying asset. Hence, if investors believe the price of such an asset will increase [but not too much], it can be a method of decreasing the cost of entering into a call option contract.

5.2   Monte Carlo Pricing Scheme

For each barrier level (B) we simulate a large number of possible price paths (200000) under a GBM model with the parameters given in Q1.
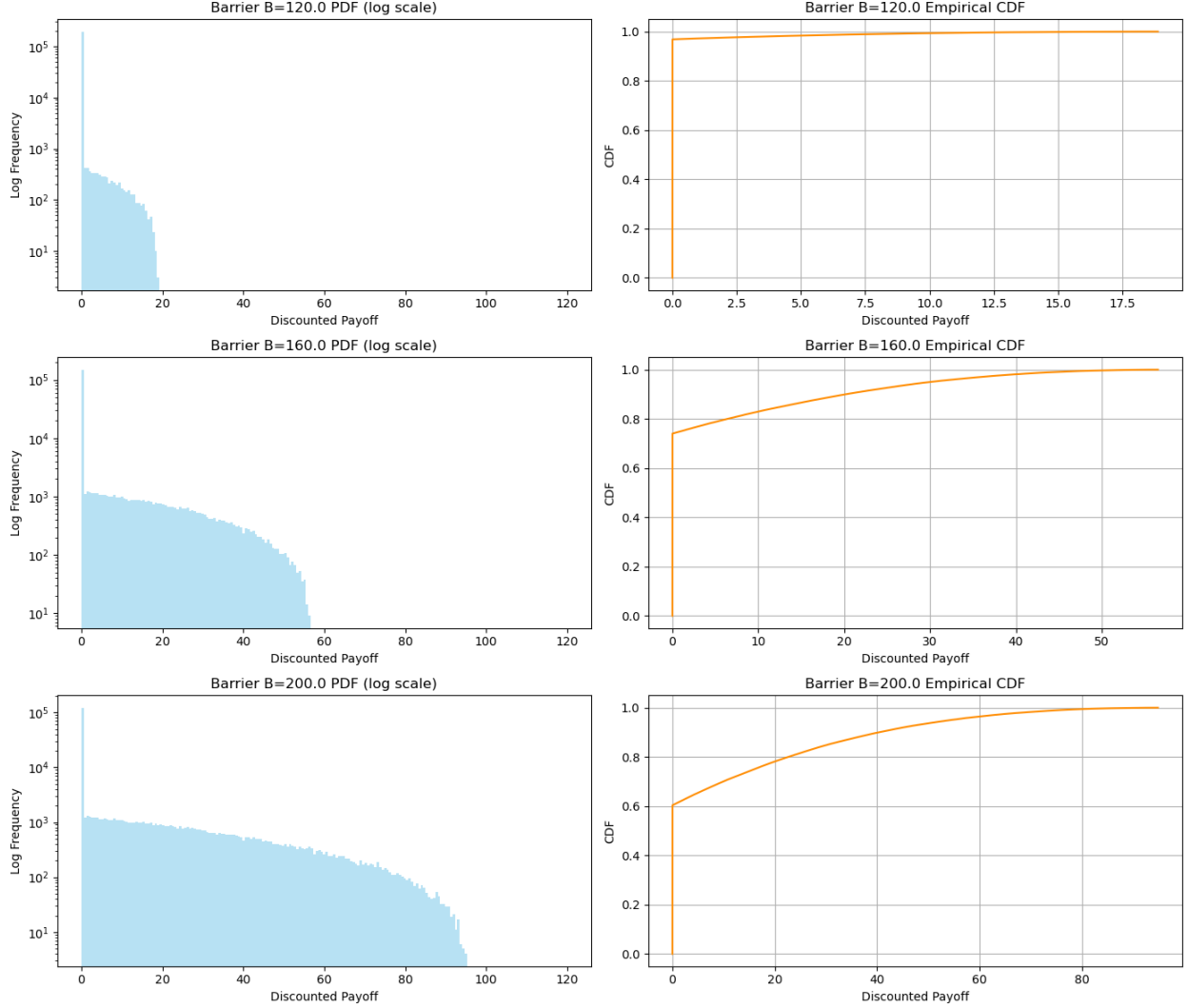

Figure 10: **Left**: Log-scaled histogram detailing the distribution of discounted payoffs for the up-and-out call based on different barrier levels (B). **Right**: Empirical cumulative distribution function (CDF) of the same payoffs.

Based on how the up-and-out call is defined, we can infer that the supremum of the undiscounted payoff is $B - K = B - 100$, $\forall B > K$. Thus, no frequencies recorded after this value is expected. We can see that the payoff distributions are right skewed with a large mass at zero across all barrier levels (B). However, as we increase the barrier level, the distribution becomes less right skewed and the mass at 0 decreases. This is intuitive. If the barrier level is close to the initial price S_0, it is very likely that it will eventually surpass or touch it before the option matures. This is also why up-and-out call options with lower barrier levels (on the same underlying) are cheaper than those with higher barriers.

Table 17: Up-and-out call Monte Carlo estimates for different barrier levels B.

B	MC Price	Std. Error	95% CI
120	0.190979	0.002959	[0.185180, 0.196778]
160	4.650944	0.022945	[4.605973, 4.695915]
200	10.835384	0.041783	[10.753491, 10.917278]

5.3 Analytic Price (Barrier Option Formula)

We can define the up-and-out call option in terms of its complimentary option, the up-and-in. The up-and-in call option only becomes alive when the price of the underlying asset touches or exceeds a given barrier (B). In a sense, it can be thought of as the opposite of the up-and-out. Its payoff bracket can be represented as:

$$\text{Payoff} = \begin{cases} (S_T - K)^+, & \text{if } \max_{0 \leq t \leq T} S_t \geq B, \\ 0, & \text{otherwise.} \end{cases}$$

When $B \geq K$, the closed analytic solution for the price of the up-and-in call option is,

$$c_{\text{ui}} = S_0 e^{-qT} N(x_1) - K e^{-rT} N(x_1 - \sigma\sqrt{T}) - S_0 e^{-qT} \left(\frac{B}{S_0}\right)^{2\lambda} [N(-y) - N(-y_1)]$$

$$+ K e^{-rT} \left(\frac{B}{S_0}\right)^{2\lambda - 2} \left[N(-y + \sigma\sqrt{T}) - N(-y_1 + \sigma\sqrt{T})\right].$$

The following parameters are defined as such:

$$\lambda = \frac{r - q + \frac{1}{2}\sigma^2}{\sigma^2}, \; x_1 = \frac{\ln\left(\frac{S_0}{B}\right)}{\sigma\sqrt{T}} + \lambda\sigma\sqrt{T},$$

$$y = \frac{\ln\left(\frac{B^2}{S_0 K}\right)}{\sigma\sqrt{T}} + \lambda\sigma\sqrt{T}, \; y_1 = \frac{\ln\left(\frac{B}{S_0}\right)}{\sigma\sqrt{T}} + \lambda\sigma\sqrt{T}.$$

Finally the price of the up-and-out call can be represented as:

$$c_{\text{uo}} = c - c_{\text{ui}}$$

where c is the price of a vanilla European call option.

5.4 Numerical Comparison: Monte Carlo vs Analytic

We compare the Monte Carlo estimates with the closed-form barrier option price for selected parameter sets. Notice that the Monte Carlo estimates are very close to the analytic price; this is also shown in the relative error. Therefore, we are confident that with enough time steps, and over many simulations, the MC estimate converges to the analytic price for the up-and-out call option. Mathematically, the MC estimate and the analytic price are calculating the same expectation. The sample price which is calculated by the Monte Carlo scheme is an unbiased estimator of the true analytic price. The Law of Large Numbers guarantees that the MC price converges almost surely.

$$\hat{C}_N \xrightarrow{a.s} C_{analytic}$$

Table 18: Up-and-out call price – analytic vs Monte Carlo for given B.

B	Analytic Price	MC Estimate	Std. Error	Relative Error
120	0.196395	0.190979	0.002959	0.027577
160	4.675802	4.650944	0.022945	0.0053163
200	10.883668	10.8353844	0.041783	0.00443633

6   Conclusion

In this project we investigated the pricing and risk sensitivities of several path-dependent options under the Black–Scholes framework, with a particular focus on arithmetic- and geometric-average Asian calls and an up-and-out barrier call. Throughout, we built a common Monte Carlo engine for simulating geometric Brownian motion, validated it against known GBM moments, and used it both as a primary pricing tool and as a way to check analytic formulas drawn from the literature.

For the arithmetic-average Asian call, we first examined the basic payoff distribution and found it to be highly right-skewed with a substantial mass at zero. Despite this, the Monte Carlo estimator was stable when a sufficiently large number of paths was used. At the baseline parameters, the control-variate estimator produced a tight confidence interval and a variance reduction of over two orders of magnitude relative to the raw estimator. Parameter sweeps over S_0, K, σ, r, T, and the monitoring frequency m all behaved in line with financial intuition: prices increased in S_0, σ, r, and T, decreased in K, and declined (to a limiting value) as the monitoring grid was refined. These experiments confirmed both the correctness of the implementation and the qualitative similarities and differences between Asian and vanilla European calls.

We then studied time-discretization effects using three schemes introduced in the course: Euler–Maruyama, Milstein, and a second-order weak Taylor method. On the test problem, all three schemes produced prices close to a high-accuracy "exact-step" benchmark, but the weak second-order scheme exhibited the smallest bias, as expected from its higher weak convergence order. This illustrates how discretization choices can introduce systematic errors in option pricing, even when Monte Carlo noise is small, and motivates the use of exact GBM steps whenever they are available.

In the Greeks analysis for the arithmetic Asian call, we implemented both pathwise and finite-difference estimators for Δ, vega ν, and ρ, using antithetic variates and common random numbers. The two approaches agreed to within one or two standard errors across a range of bump sizes, and FD–PW z-scores stayed comfortably inside the usual $|z| \leq 1.96$ band. Standard errors scaled almost exactly like $N^{-1/2}$ when the number of paths was doubled, confirming the expected Monte Carlo convergence. Overall, the pathwise estimator was particularly convenient and precise for Δ, while CRN made finite differences competitive for all three Greeks without any noticeable bias.

For the geometric-average Asian call, we derived the distribution of the log-geometric average under GBM, showed that it is Gaussian, and obtained a Black–Scholes–style closed form in terms of effective parameters (μ_G, σ_G^2) or, equivalently, an effective dividend yield q_G. The resulting analytic price was then checked against a Monte Carlo estimate at the same baseline parameters; the closed-form value lay well within the 95% confidence interval of the simulation, with a relative error of well under 1%. This provides a strong consistency check for both the derivation and the implementation, and also justifies the use of the geometric Asian as a natural control variate for the arithmetic Asian.

Finally, for the up-and-out barrier call we described the contract, implemented a Monte Carlo pricing scheme, and compared the results to a standard closed-form barrier option formula expressed via an up-and-in call and put–call-type decompositions. Across several barrier levels, the Monte Carlo prices were very close to the analytic values, with small relative errors and confidence intervals that easily covered the theoretical prices. The payoff distributions showed the expected heavy mass at zero and strong right skewness, especially for low barriers, and the option price increased towards the vanilla European call price as the barrier was moved further away.

Taken together, these results demonstrate that a carefully implemented Monte Carlo framework, combined

with variance-reduction techniques, pathwise and finite-difference Greeks, and appropriate discretization schemes, can provide accurate and interpretable prices and sensitivities for a range of path-dependent options. At the same time, the work highlights some limitations of the Black–Scholes setting (constant volatility, lognormal dynamics, and idealised monitoring) and suggests natural extensions, such as stochastic volatility models, quasi–Monte Carlo sampling, or more sophisticated variance reduction, which could further improve realism and computational efficiency in practical applications.

7 References

- Hull, J. C. (2022). Options, Futures, and Other Derivatives (11th ed.). Pearson Education.
- Glasserman, P. (2004). Monte Carlo Methods in Financial Engineering. Springer.